

*promoting access to White Rose research papers*



**Universities of Leeds, Sheffield and York**  
**<http://eprints.whiterose.ac.uk/>**

---

This is an author produced version of a paper published in **Journal of the Energy Institute**

White Rose Research Online URL for this paper:

<http://eprints.whiterose.ac.uk/id/eprint/77991>

---

**Paper:**

Illingworth, J, Williams, PT and Rand, B (2013) *Characterisation of biochar porosity from pyrolysis of biomass flax fibre*. Journal of the Energy Institute, 86 (2). 63 - 70. ISSN 1743-9671

<http://dx.doi.org/10.1179/1743967112Z.00000000046>

---

## Characterisation of Biochar Porosity from the Pyrolysis of Biomass Flax Fibre

**James Illingworth<sup>#</sup>, Paul T. Williams<sup>#\*</sup> and Brian Rand<sup>+</sup>**

*Energy Research Institute<sup>#</sup> and Institute for Materials Research<sup>+</sup>,*

*University of Leeds, Leeds LS2 9JT, UK*

### **Abstract**

Low grade biomass fibre produced as a by-product from the flax industry was manufactured into a non-woven fabric. This material was then pyrolysed in a fixed bed reactor to produce biochar. The resulting biochars were characterised using a variety of techniques including gas adsorption, scanning electron microscopy, pycnometry and elemental and proximate analyses. The fibrous morphology of the precursor was retained during pyrolysis. The temperature of pyrolysis had a significant influence on the biochar properties, with higher temperatures causing an increase in surface area and density along with a decrease in volatile/disorganised carbon. All of the biochars were microporous, with the majority in the ultramicropore size range. Activated diffusion effects were observed during nitrogen adsorption measurements at 77K. The experimental data show that the flax biochars exhibit properties typical of biochars produced from other lignocellulosic precursors.

Key Words: Biomass; waste; pyrolysis; carbon

\* Corresponding author; p.t.williams@leeds.ac.uk

## **Introduction**

Historically, the most common applications for biomass fibres such as flax were in the production of yarns and rope, which were used for fishing, construction, clothing and binding.<sup>1</sup> Throughout the 20<sup>th</sup> Century however, the use of natural fibres has declined due to the availability of a wide range of synthetic fibres produced from petrochemical precursors.<sup>2</sup> However, more recently, concern over the extensive consumption of finite resources has prompted greater interest in the use of renewable biomass materials. This is expected to provide a positive stimulus to the natural fibre market, with respect to traditional end-uses such as textile production, and also in the development of new technologies to replace synthetic fibres in reinforced composites, packaging materials, thermal insulation, filters and absorbents.<sup>2</sup> Textile materials derived from natural biomass fibres can utilise less than 50% by weight of such fibres in production, thereby producing a high proportion of waste.

A particular advantage of such fibrous textile waste is that the biomass material has a fibrous characteristic enabling the fibres to be processed to produce a fabric non-woven matting material. Because of the strength of the flax fibres, they can easily undergo the entanglement, layering and needling which produces a non-woven matting product.

Biomass fibres are classified as lignocellulosic materials, consisting predominantly of cellulose, hemi-cellulose and lignin. A wide variety of other lignocellulosic materials have been pyrolysed to produce end-product char, oil or gas including various nutshells, wood, rice straws and fruit stones.<sup>3-10</sup> However, the morphology of biomass fibre potentially offers significant advantages over other lignocellulosic materials.

Biochar is a recent term used to describe the chars produced from biomass but with the particular end-use of a soil enhancer. Biochar also improves water quality and quantity

by increasing soil retention of nutrients and agrochemicals for plant and crop utilization. More nutrients stay in the soil instead of leaching into groundwater and causing pollution. The biochars for such applications tend to be fine grained and are added to soil to hold the carbon from the original biomass in the soil and therefore act as a carbon sequestration process. The processing of biomass waste into a non-woven fabric matting material which is then pyrolysed to produce a carbonaceous biochar matting represents a novel form of biochar for different potential applications.

This paper investigates the influence of pyrolysis temperature on the yield and composition of the products of pyrolysis of non-woven flax fibre material. The yield of biochar, liquid and gas in relation to temperature are reported and the detailed characterization of the product biochars in terms of their structural characteristics, surface area and porosity are described.

## **Materials and Methods**

### **Flax Fibre Precursor Material**

The precursor material consisted of low-grade flax fibre obtained from British Fibres Limited, a company funded by the Engineering and Physical Sciences Research Council (EPSRC) and the UK Ministry of Agriculture, Fisheries and Food (now the Department of the Environment, Food and Rural Affairs). The characteristics of the raw fibre are reported in Table 1. The 'as-received' raw fibre was then converted into a non-woven fabric (Figure 1) involving a sequential process consisting of a dry laid carded method, needle punch bonding and calender bonding. The process of dry laid carding involves the use of rotating cylinders

covered in wires or teeth that arrange the fibres into parallel arrays of up to 150 mm fibre length and a thickness of 8 mm. The fibre material is then needle punched which involves punching of barbed needles through the material, hooking tufts of fibre together, this process bonds the fibres together and gives extra strength to the non-woven matting. The final process step of calender bonding involves stabilisation of the non-woven matting via heat and pressure where the fibres tend to fuse together producing a more stable structure. The final product was a roll of biomass natural fibre matting from which samples were cut for the pyrolysis experiments.

### **Thermogravimetric Analysis of Flax Fibre**

Initial characterization of the flax fibre non-woven fabric material was investigation using a thermogravimetric analyser to determine the weight loss characteristics of the sample in relation to increasing temperature and hence the appropriate pyrolysis temperatures for the subsequent pyrolysis experiments. The weight loss behaviour of the flax fibre was studied using a Stanton-Redcroft thermogravimetric analyser (TG 760 series). Approximately 20mg of sample was used for the analysis with a heating rate of  $10^{\circ}\text{C min}^{-1}$ . The TGA furnace was purged with an atmosphere of nitrogen throughout the analysis.

### **Pyrolysis of Flax Fibre**

The non-woven fibrous material was pyrolysed in a vertical-tube fixed bed reactor, a schematic diagram of which is shown in Figure 2. The tube was constructed of stainless steel of 65 mm diameter and 200 mm length, and was heated by an electrical ring furnace. The reactor was continuously purged with nitrogen at a metered flow rate of  $300\text{ml min}^{-1}$ . A sample of 60g of biomass material was placed on a support in the centre of the hot-zone of

the reactor and was heated at a controlled rate of  $2^{\circ}\text{C min}^{-1}$  to the desired final temperature with a hold time at each temperature of 60 minutes. The resulting biochar was then weighed and stored under nitrogen prior to further analysis. The liquid fraction produced during the pyrolysis experiments was collected in a series of dry-ice cooled condensers and the yield determined gravimetrically. The yield of gaseous products was calculated by difference.

### **Characterization of Flax Fibre and Biochars**

The pore structures of the flax precursor and resulting biochars were characterised by physical adsorption of gases, using a Quantachrome Autosorb 1-C Instrument. All chars were outgassed prior to analysis using a staged outgassing procedure. Firstly, the sample was held under vacuum at room temperature for 30 minutes, followed by 60 minutes at  $105^{\circ}\text{C}$ . Finally, the temperature was raised to  $250^{\circ}\text{C}$  and maintained overnight. The raw flax samples were outgassed at  $50^{\circ}\text{C}$  for 24 hours to avoid the potential decomposition of the material at elevated temperatures.

Adsorption isotherms of  $\text{N}_2$  were determined over a range of relative pressures from  $1 \times 10^{-6}$  up to 0.995. The desorption branch of the isotherm was measured back down to a partial pressure of 0.10. The surface area ( $A_{\text{BET}}$ ) of the samples was calculated using the BET method and total micropore volume ( $\text{DR-N}_2$ ) using the Dubinin-Radushkevitch equation (pore size  $<2\text{nm}$ ). The mesopore volume ( $V_{\text{MES}}$ ) was determined using the method described by Rodriguez-Reinoso *et al.*<sup>11</sup> and the single point total pore volume ( $V_{\text{TOT}}$ ) was calculated from the amount of nitrogen adsorbed at the relative pressure of 0.98.

Adsorption isotherms of  $\text{CO}_2$  were produced over the relative pressure range  $1 \times 10^{-6}$  to 0.03. The Dubinin-Radushkevitch equation was used to provide an assessment of the volume of narrow micropores ( $\text{DR-CO}_2$ ) (pore size  $<0.7\text{nm}$ ). Micropore size distribution

plots were constructed using the Density Functional Theory (DFT) software supplied by Quantachrome.

The moisture, ash and volatile matter content of the raw flax fibre and resulting biochars was determined according to the solid fuel proximate analysis (BS1016 part 3) with the result given as the mean of three determinations. A Carbolite nitrogen-purged moisture oven and three Carbolite muffle furnaces were used for the analysis. The fixed carbon content was determined by difference from the moisture, ash and volatile matter tests.

Elemental analysis (C, H, N, S, O) of the samples was carried out using an elemental analyser (CE Instruments Flash EA 1112). Sample sizes were in the range 3-5mg. As for the proximate analysis, the result was taken as the mean of three determinations.

The true density of the samples was determined by helium displacement (Micromeritics Accupyc 1330) and the bulk and apparent densities by mercury intrusion porosimetry (Micromeritics Poresizer 9320).

The surface morphology of the biochars was investigated using a LEO 1530 Field Emission Gun, High Resolution SEM. The instrument was operated with a working distance of 6 to 8mm and an accelerating voltage of 2 to 3kV using the in-lens detector. Specimens were coated with a 3nm layer of platinum using an Agar High Resolution Sputter Coater and stored in a dessicator prior to analysis.

The repeatability of the experimental and analytical procedures was verified by repeat experiments of pyrolysis through to the characterisation of the resulting biochars. The reproducibility of the work was found to be excellent. In addition, the accuracy of the analytical techniques was determined using standard materials.

## Results and Discussion

### Thermogravimetric Analysis of Flax Fibre

The pyrolytic decomposition of the flax fibre in the thermogravimetric analyser began at about 250°C and rapid weight loss was observed up to around 450°C. The mass of char at this stage constituted around 29% of the original biomass. There was then a steady, more gradual decline in mass up to the final temperature with a final char yield of just below 20% of the original dry biomass. The carbonisation process is a complex reaction system involving the elimination of volatile products and structural re-organisations within the remaining solid phase. For cellulose<sup>12</sup> (the major constituent of natural fibres), the first stages involve the elimination of physically held water at <300°C, with some re-arrangement of structure within the cellulose. Later, structural water is evolved from hydrogen and hydroxyl groupings in the cellulose lattice. Between 240 and 400°C, splitting of C-O and C-C bonds occurs with production of tars, water, carbon monoxide and carbon dioxide. It is these reactions which result in the rapid weight loss observed between 250 and 450°C for the flax fibre.

The weight loss behaviour of flax fibre during pyrolysis appears to be similar to other lignocellulosic materials. Byrne and Nagle<sup>13</sup> pyrolysed red oak in a TGA and found the majority of the weight loss had occurred prior to 450°C. Williams and Besler<sup>14</sup> pyrolysed rice husks and found similar results, with the main weight loss complete by 500°C.

### Pyrolysis Product Yield

As a consequence of the TGA data, final pyrolysis temperatures of 500, 650, 800 and 950°C were used to investigate the influence of pyrolysis temperature on biochar characteristics. Figure 3 shows the pyrolysis mass balance for the carbonisation of flax at different

temperatures. The product mass balances for the samples can be considered to be fairly similar over the studied range of temperature. The liquid fraction was the largest product, although similar in yield there was an indication of increasing liquid yield from 53.6 wt% at 500°C up to 55.6 wt% at 950°C. The liquid consisted of an oil and an aqueous phase. The yield of gaseous products also increased slightly between 500 and 950°C. The trends observed for the liquid and gaseous fractions have been observed in other studies of biomass pyrolysis.<sup>4,14</sup> Conversely, other workers have observed an initial increase in the liquid product with temperature, followed by a decline as the temperature was further increased. Maschio *et al.*<sup>15</sup> noted a decrease in oil yield above 400°C accompanied by a large increase in the gaseous fraction, whereas Figuieredo *et al.*<sup>16</sup> observed similar results at temperatures in excess of 500°C. Maschio *et al.*<sup>15</sup> suggested that the enrichment of the gaseous phase due to the breakdown of larger molecules in the liquid fraction was responsible for this phenomenon.

In contrast to the gas and liquid fractions, the biochar yield declined with increasing temperature, with 25.1wt% at 500°C falling to 21.5wt% at 950°C. The biochar yields observed from the fixed bed reactor are somewhat higher than those indicated by the TGA analysis (~20 wt% after 1 hour), despite the inclusion of a hold period in the fixed bed experiments. This is likely to be a feature of the lower heating rates used in the fixed bed reactor as it is recognised that lower heating rates lead to an increase in the yield of char during pyrolysis.<sup>12, 17-18</sup> The reported char yield values are within the range reported by other studies in the literature.<sup>4, 12, 15</sup>

### **Morphology of Flax and Flax Biochars**

Figure 4(a) and 4(b) show scanning electron micrographs (SEM) of the original flax fibre at x5,000 and x100,000 magnification respectively. It is apparent that the fibre surface is uneven and has a striated texture, with parallel ridges of width around 50nm running along the length. These ridges may be related to the parallel arrangement of the cellulose microfibrils in the secondary cell wall.<sup>19</sup> Figure 4(b) also shows the presence of surface agglomerations of sub-micron dimensions. The outer layer of biomass fibres is known as the cuticle (or middle lamella) and is made up of lignin, pectin and waxes. The purpose of this outer layer is to bind the individual fibres into bundles within the bast layer of the parent plant. Thus, it seems likely that the micrographs are showing the cuticle of the fibres, the surface agglomerations possibly consisting of pectin and/or lignin from the original fibre bundles. The SEM images show no evidence of a pore structure within the raw flax fibre.

Figure 5 shows a photograph of the pyrolysis biochar produced after pyrolysis of the flax non-woven fabric material at 800°C. The flax biochars maintained the non-woven fibrous form of the original flax material over the whole range of pyrolysis temperatures studied. The flexibility of the material was also maintained.

Figure 6(a) shows a scanning electron micrograph of the pyrolysis biochar produced from flax pyrolysis at 800 °C at a magnification of x12,000 and Figure 6(b) shows the biochar fibre surface at x200,000 magnification. Figure 6(a) shows the fibre-ends of the carbonized material. Hollow channels in the macropore size range may be seen running through the centre of the fibres. These channels constitute the lumen, a central channel of hollow space which is part of the nutrient transport system of the parent plant.<sup>20</sup> The lumen was not visible during SEM examination of the raw flax fibre, presumably due to the presence of dried protoplasmic residues within the ducts.<sup>20</sup> Figure 6(b) shows that there is little evidence of the presence of a well developed pore structure on the surface of the fibres,

although a small number of slit shaped cracks in the mesopore size range are visible. This agreed with the gas adsorption data (later) which indicated that the pore structure of the biochars consists mainly of ultramicropores with little in the way of larger porosity. Such tiny pores ( $<10\text{\AA}$ ) are beyond the resolution of the SEM.

### **Physical and Chemical Properties of Flax Biochars**

The biochars derived from the pyrolysis of flax fibre were analysed for a range of properties, including the elemental and proximate analysis, bulk, apparent and true density. The results are shown in Table 2. The main feature of the proximate analysis data was the reduction in volatile matter content and increase in fixed carbon as the temperature of pyrolysis was increased. This was particularly marked between the raw flax and the  $500^{\circ}\text{C}$  biochar with the volatile matter reducing from 75.6wt% to 25.7wt% and fixed carbon increasing from 15.2 to 65.8wt%. This is due to the devolatilisation of the flax during the main period of weight loss between  $275$  and  $450^{\circ}\text{C}$ , where the majority of the volatile matter is released in the tar and gaseous fractions. As the pyrolysis temperature was increased further, the volatile matter content reduced more steadily. The ash content of the biochars also increased with increasing temperature, indicating that the majority of the inorganic components present in the original fibre remain in the biochar structure and are not released during pyrolysis.

The elemental analysis shows that the carbon content of the samples increased with temperature whereas the proportion of hydrogen and oxygen was considerably reduced, indicating a more aromatic carbon structure. In each case, the main changes take place up to  $500^{\circ}\text{C}$ . The solid biochar is rich in carbon due to the elimination of heteroatoms via the gaseous and liquid fractions. The carbon atoms are grouped into stacks of aromatic sheets and strips cross-linked in a random manner. Since the arrangement of these sheets is irregular, it

leaves free interstices among them which constitute a rudimentary pore structure. However, the pore structure of the chars is often blocked by tars and other pyrolytic decomposition products which become disorganized carbon.

Table 2 also shows a clear trend of increasing density with temperature. This is likely to be due to a combination of factors such as the removal of lighter volatile material, the increasing ash component and the densification of the carbon matrix.<sup>21</sup> The values obtained are similar to those obtained by other workers studying the pyrolysis of biomass.<sup>21-22</sup>

### **Porous Texture of Flax Fibre Biochars**

#### ***Nitrogen Adsorption Isotherms***

The raw flax and biochars were characterised by adsorption of nitrogen at 77K and the adsorption isotherms are presented in Figure 7. The isotherm for the raw flax shows limited adsorption and is characteristic of a non-porous solid (type II isotherm). The adsorption capacity of the chars increases with pyrolysis temperature and significant uptake of nitrogen occurs at very low relative pressures, indicating the presence of micropores. The most striking feature of the N<sub>2</sub> isotherms is the presence of significant 'low-pressure hysteresis', which is related to the entrapment of adsorbate molecules in very fine ultramicropores with dimensions close to those of the adsorbate.<sup>23</sup> Nitrogen adsorption on carbon materials containing a high proportion of ultramicropores<sup>24,25</sup> is difficult and has been attributed to diffusional limitations of nitrogen at 77K into fine micropores of molecular dimensions. Garrido *et al.*<sup>26</sup> and Thakur and Brown<sup>25</sup> have shown that difficulties with nitrogen adsorption measurements due to the presence of fine micropores may be overcome by using CO<sub>2</sub> adsorbate at 273K. At this temperature, CO<sub>2</sub> molecules can more easily access

ultramicropores than N<sub>2</sub> at 77K in spite of the fact that the critical molecular dimensions of both gases are similar.<sup>26</sup>

### ***Carbon Dioxide Adsorption Isotherms***

The porous structure of the raw flax and biochars was studied by adsorption of carbon dioxide at 273K. It was hoped to remove the problems associated with the adsorption of nitrogen at 77K and more accurately assess the presence of ultramicropores in the samples. The adsorption isotherms and the DFT micropore size distributions are presented in figure 8 and figure 9 respectively. Porous texture data for both CO<sub>2</sub> and N<sub>2</sub> adsorbates are presented in table 3.

The CO<sub>2</sub> isotherms and corresponding DFT plots show the presence of considerable microporosity in the flax chars. This is present in the form of ultramicropores, predominantly with width less than 6Å. These pores appear to be formed during the carbonisation process as they are absent in the raw flax precursor, which shows little adsorption of CO<sub>2</sub>. As the carbonisation temperature is increased from 500 to 800°C, the narrow micropore volume (DR-CO<sub>2</sub>) increases slightly before showing a slight decline between 800 and 950°C. The overall shape of the DFT plots remains similar between 500 and 800°C, with the creation of narrow micropores a feature. The peak at 3-4Å increases considerably, with a smaller increase in the peak between 4 and 7Å also noted. At 950°C, considerable widening of the narrow micropores has occurred with the 3-4Å peak much reduced but an increase and broadening of the 4-7Å peak. The contribution of pores in excess of 8Å has also increased considerably.

This is reinforced by the DR values and isotherms for the two adsorbates which also indicate a widening of the micropores with increasing temperature. However, the micropore

volume determined by CO<sub>2</sub> is considerably greater than the N<sub>2</sub> value for all carbonised samples. This highlights the problems of N<sub>2</sub> adsorption at low temperatures for ultramicroporous samples and confirms that access to the narrow micropores is influenced by diffusional limitations. It is likely that this is a result of the partial blockage of micropore entrances by disorganised material deposited during the pyrolysis process. These constrictions are then responsible for the low pressure hysteresis identified in figure 7. This is further demonstrated for the 950°C char, which has a wider pore size distribution and less significant low-pressure hysteresis. The higher temperature of pyrolysis helps remove tarry and disorganised matter, thus removing constrictions and creating a more accessible pore structure. Other workers have found similar results when characterising the pore structure of chars with a high proportion of ultramicropores. Wynne-Jones and Marsh<sup>27</sup> pyrolysed a series of organic polymers at different temperatures. The samples were analysed by adsorption of N<sub>2</sub> at 77K and CO<sub>2</sub> at 195K. In all cases, the N<sub>2</sub> isotherms led to much lower values of surface area than did the carbon dioxide isotherms and was attributed to the higher temperature of measurement facilitating entry to the fine micropores. Rubio and Izquierdo<sup>28</sup> found similar trends in a series of low-rank coal chars. As in the current work, both studies showed the greatest differences at lower pyrolysis temperatures, with accessibility to the N<sub>2</sub> adsorbate improving at higher temperatures. Gregg *et al.*<sup>29</sup> examined uptake of butane at different temperatures on the same microporous carbon. As the adsorption temperature was increased from 196 to 273K, a dramatic increase in the adsorption capacity was observed.

### ***Pore Volume by Pycnometry***

The presence of very fine micropores in the flax biochars was further demonstrated by means of the helium and mercury density measurements. Using equation 1, an assessment of the

pore volume of the chars accessible to helium but inaccessible to mercury can be made (ie. pore sizes below 3.54nm).

$$V = (1/\rho_{\text{Hg}}) - (1/\rho_{\text{He}}) \quad (1)$$

where:  $V$  = volume of pores of width  $<3.54\text{nm}$  ( $\text{cm}^3/\text{g}$ )

$\rho_{\text{He}}$  = Helium density ( $\text{g}/\text{cm}^3$ )

$\rho_{\text{Hg}}$  = Mercury density ( $\text{g}/\text{cm}^3$ )

The values obtained could then be compared directly with the pore volumes determined from the gas adsorption data (Table 3). The data are shown in figure 10. The most interesting feature of these data is the difference between the three sets of values. For all biochars, the volume determined by pycnometry is greater than that determined by either  $\text{CO}_2$  or  $\text{N}_2$  adsorption. This suggests the presence of a large number of micropores inaccessible to  $\text{CO}_2$  or  $\text{N}_2$ , but accessible to helium, the helium atom being of considerably smaller size ( $2.58\text{\AA}$ ).<sup>30</sup> The difference between the values decreases with increasing pyrolysis temperature, suggesting that the pore structure becomes more accessible to larger molecules. This was also indicated by the gas adsorption data.

Figure 10 also shows conflicting trends regarding the development of porosity as a function of pyrolysis temperature. The pore volume determined by pycnometry declines with increasing temperature, whereas the gas adsorption data show the reverse trend. A trend of increasing surface area and pore volume with temperature is a common feature during the pyrolysis of non-graphitizing carbons.<sup>21,27,31-32</sup> It is also well established that an optimum temperature exists where the pore volume/surface area reaches a maximum value, before

declining with further increases in temperature. However, the temperature at which the maximum is observed varies widely and is dependant on the initial precursor. Wynne-Jones and Marsh <sup>27</sup> studied the pyrolysis of organic polymers at temperatures up to 1000°C. Gas adsorption data from the resulting biochars showed a wide variation in the temperature at which the maximum surface area was obtained. For example, dibenzanthrone carbons showed a maximum at <600°C, whereas for polyfurfuryl chars the maximum occurred at 800°C. Masters and McEnaney <sup>31</sup> pyrolysed cellulose pellets and found the micropore volume of the chars increased steadily up to 1000°C, followed by a rapid decline thereafter. The same paper attributed the decline in porosity to shrinkage of the char structure and the 'conversion of open micropores to closed micropores via the progressive narrowing of ultramicroporous layer spacings'. It seems probable that the increased aromatic nature of the chars, together with structural shrinkage, is responsible for the conflicting trends in figure 10.

## **Conclusions**

A non-woven fabric was produced from biomass fibre obtained as a waste product from the flax industry. The material was pyrolysed in a fixed bed reactor at various temperatures. The fibrous morphology and flexibility of the precursor material was retained during pyrolysis. Increasing temperature of pyrolysis from 500 °C to 950 °C showed that the main product was liquid with a yield of ~54 wt% and the biochar ranged from 25.1 wt% at 500 °C to 21.5 wt% at 950 °C. The biochars were characterized using a range of analytical techniques and were found to exhibit properties typical of those obtained from other lignocellulosic materials. Scanning electron microscope analysis of the biochars showed the presence of the original

structure of the flax. Detailed characterization of the biochars showed that they were mainly microporous with the majority being in the range of ultramicropores.

## References

- [1] S.K. Batra, 'Other Long Vegetable Fibres'. In: Lewin, M. and Pearce, E.M. (eds) *Handbook of Fibre Chemistry*, 1998, Marcel Dekker, New York.
- [2] P.O. Olesen and D.V. Plackett, *Perspectives on the performance of natural plant fibres*. Report of the Plant Fibre Laboratory, 1998, Royal Veterinary and Agricultural University, Copenhagen, Denmark.
- [3] P.T. Williams and A.R. Reed. *J. Anal. Appl. Pyrol.*, 2003, **70**, 563-577.
- [4] A.R. Reed and P.T. Williams, *Int. J. Energ. Res.*, 2004, **28**, 131-145.
- [5] R. Isha and P.T. Williams, *J. Energ. Inst.* 2011, **84**, 80-87.
- [6] W.K. Buah, A.M. Cunliffe and P.T. Williams, *Proc. Saf. Environ*, 2007, **85**, 450-457.
- [7] P.T. Williams and N. Nugranad N. *Energy*, 2000, **25**, 493-513.
- [8] G. Oh and C.R. Park, *Fuel*, 2002, **81**, 327-336.
- [9] P.T. Williams and S. Besler, *Renew. Energ.*, 1996, **7**, 233-250.

- [10] H. Marsh, M. Iley, J. Berger and T. Siemiensiewska, *Carbon*, 1975, **13**, 103-109.
- [11] F. Rodriguez-Reinoso, M. Molina-Sabio and M.T. Gonzalez, *Carbon*, 1995, **33**, 15-23.
- [12] A.C. Pastor, F. Rodriguez-Reinoso, H. Marsh and M.A. Martinez, *Carbon*, 1999, **37**, 1275-1283.
- [13] C.E. Byrne and D.C. Nagle, *Carbon*, 1997 **35**, 259-266.
- [14] P.T. Williams and S. Besler, *Fuel*, 1993, **72**, 151-159.
- [15] G. Maschio, C. Koufopoulos and A. Lucchesi, *Biores. Technol.*, 1992, **42**, 219-231.
- [16] J.L. Figueiredo, C. Valenzuela, A. Bernalte, and J.M. Encinaar, *Fuel*, 1989, **68**, 1012-1016.
- [17] P.H. Brunner and P.V. Roberts, *Carbon*, 1980, **18**, 217-224.
- [18] P.T. Williams and S. Besler, *Energy*, 1996, **7**, p.233-250.
- [19] P.T. Williams and A.R. Reed, *Biomass Bioenerg.*, 2006, **30**, 144-152.

[20] T.P. Nevell and S.H. Zeronian, *Cellulose chemistry and its applications*, 30-41, 1985, Ellis Harwood Ltd., Chichester.

[21] T.K. Gale, T.H. Fletcher, and C.H. Bartholomeus, *Energ. Fuel.*, 1995, **9**, 513-524.

[22] J. Guo and A.C. Lua, *J. Anal. Appl. Pyrol.*, 1998, **46**, 113-125.

[23] S.J. Gregg and K.S.W. Sing, *Adsorption, Surface Area and Porosity*. 1982, Academic Press, London.

[24] F. Rodriguez-Reinoso and A. Linares-Solano, In: Thrower, P.A. (Ed) *Chemistry and Physics of Carbon*, Vol. **21**. 1998, Marcel Dekker, New York.

[25] S.C. Thakur and L.F. Brown, *Carbon*, 1982, **20**, 17-24.

[26] J. Garrido, A. Linares-Solano, J.M. Martin-Martinez, M. Molina-Sabio, F. Rodriguez-Reinoso and R. Torregosa, *Langmuir*, 1987, **3**, 76-81.

[27] W.F.K. Wynne-Jones and H. Marsh, *Carbon*, 1964, **1**, 269-279.

[28] B. Rubio and M.T. Izquierdo *Carbon*, 1997, **35**, 1005-1011.

[29] S.J. Gregg, R.M. Olds and R.F.S. Tyson, In: *Third Conference on Industrial Carbon and Graphite*, p.184. 1970, Academic Press, London and New York.

[30] R.D. Harrison, *Nuffield Advanced Science Book of Data*, 1977, Longman Group, London.

[31] K.J. Masters and B. McEnaney, *Carbon*, 1984, **22**, 595-601.

[32] P.A. Della-Rocca, E.G. Carrella, P.R. Bonelli and A.L. Lukierman, *Biomass Bioenerg.*, 1999, **16**, 79-88.

**Table 1: Characteristics of the ‘as-received’ flax fibre**

<b>Wt. %</b>	
<i>Ultimate Analysis</i>	
Carbon	43.5
Hydrogen	6.7
Nitrogen	1.3
Oxygen (by difference)	48.5
<i>Proximate Analysis</i>	
Moisture	7.5
Volatiles	75.6
Fixed Carbon	15.2
Ash	1.7
<i>Major Components</i>	
Cellulose <sup>a</sup>	64.1
Hemi-cellulose <sup>a</sup>	16.1
Lignin <sup>a</sup>	2.0
Calorific value (MJ kg <sup>-1</sup> )	17.2
<i>Density (g cm<sup>-3</sup>)</i>	
Bulk	0.442
Apparent (Hg)	1.359
True (He)	1.369

<sup>a</sup> data from reference <sup>1</sup>

**Table 2: Characteristics of flax biochars pyrolysed at different temperatures**

Wt. %	Pyrolysis Temperature (°C)			
	500	650	800	950
<i>Ultimate Analysis</i>				
Carbon	81.2	88.6	90.3	92.6
Hydrogen	2.3	1.6	1.1	0.8
Nitrogen	2.0	1.7	0.9	0.8
Oxygen (by difference)	14.5	8.1	7.7	5.8
<i>Proximate Analysis</i>				
Moisture	2.0	1.8	1.6	2.1
Volatiles	25.2	15.8	10.4	6.7
Fixed Carbon	65.8	75.0	80.0	81.8
Ash	7.0	7.4	8.0	9.4
<i>Density (g cm<sup>-3</sup>)</i>				
Bulk	0.449	0.528	0.587	0.613
Apparent (Hg)	1.021	1.102	1.245	1.401
True (He)	1.472	1.580	1.861	1.975

**Table 3: Porous texture data for raw flax and flax biochars**

<b>Sample</b>	<b>A<sub>BET</sub> [m<sup>2</sup>/g]</b>	<b>V<sub>MIC</sub> DR-N<sub>2</sub> [cm<sup>3</sup>/g]</b>	<b>V<sub>MIC</sub> DR- CO<sub>2</sub> [cm<sup>3</sup>/g]</b>	<b>V<sub>MES</sub> [cm<sup>3</sup>/g]</b>	<b>V<sub>TOT</sub> N<sub>2</sub> [cm<sup>3</sup>/g]</b>
Flax	1.8	0.000	0.003	0.001	0.004
500°C	5.9	0.002	0.138	0.006	0.013
650°C	13.1	0.009	0.143	0.012	0.029
800°C	30.1	0.012	0.151	0.011	0.028
950°C	45.6	0.019	0.149	0.008	0.033

## Figure Captions

Figure 1. The non-woven flax fibre precursor material

Figure 2: Schematic diagram of the pyrolysis reactor

Figure 3: Pyrolysis mass balance for flax at different final temperatures

Figure 4: SEM micrograph of raw flax fibre at (a) x5000 magnification and (b) x100,000.

Figure 5: Flax non-woven fabric biochar produced at a pyrolysis temperature of 800°C

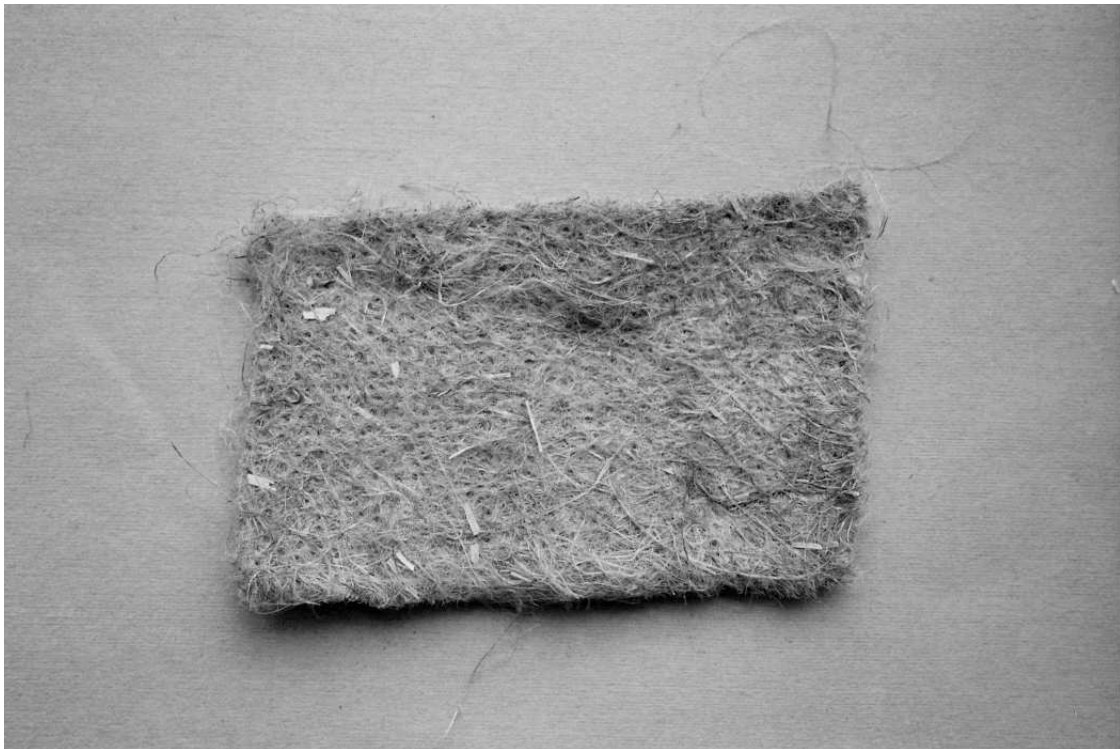
Figure 6: SEM micrograph of flax biochar fibre surface (a) x 12000 magnification and (b) x200,000 magnification

Figure 7: N<sub>2</sub> adsorption isotherms at 77K for raw flax and biochars

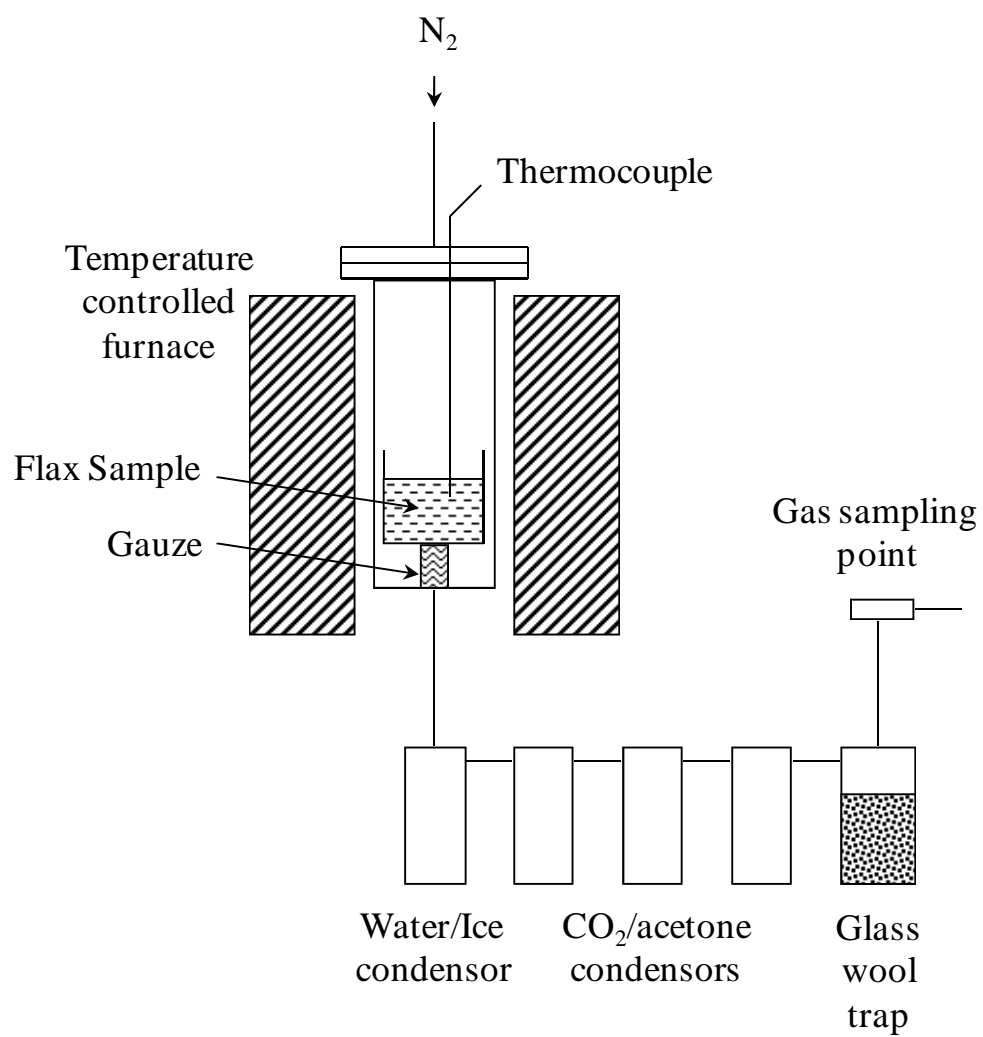
Figure 8: CO<sub>2</sub> adsorption isotherms at 273K for raw flax and biochars

Figure 9: CO<sub>2</sub> DFT micropore size distributions for raw flax and biochars

Figure 10: Comparison of pore volumes. Pycnometry vs gas adsorption



**Figure 1. The non-woven flax fibre precursor material**



**Figure 2: Schematic diagram of the pyrolysis reactor**

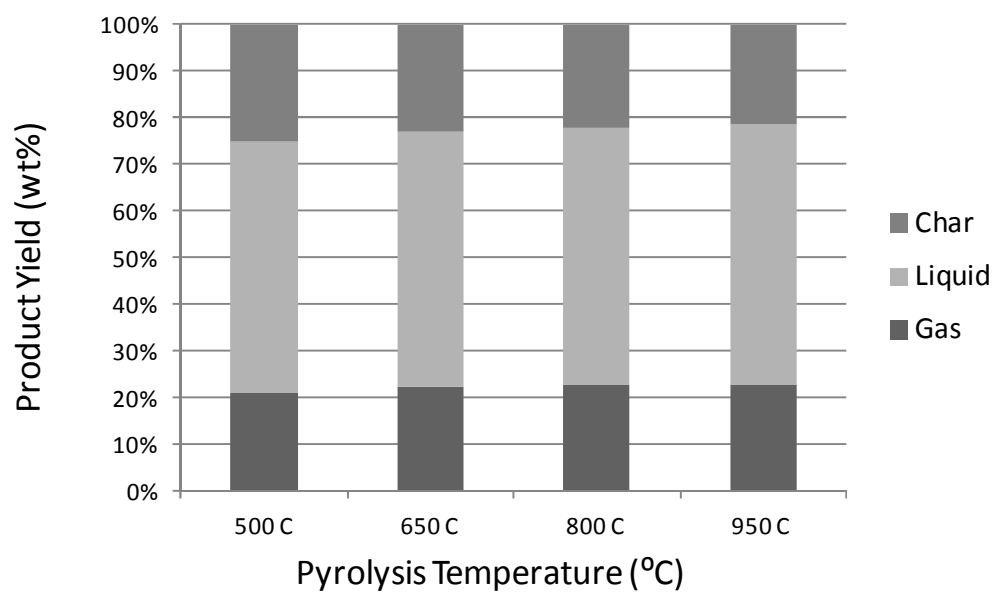


**Figure 3: Pyrolysis mass balance for flax at different final temperatures**

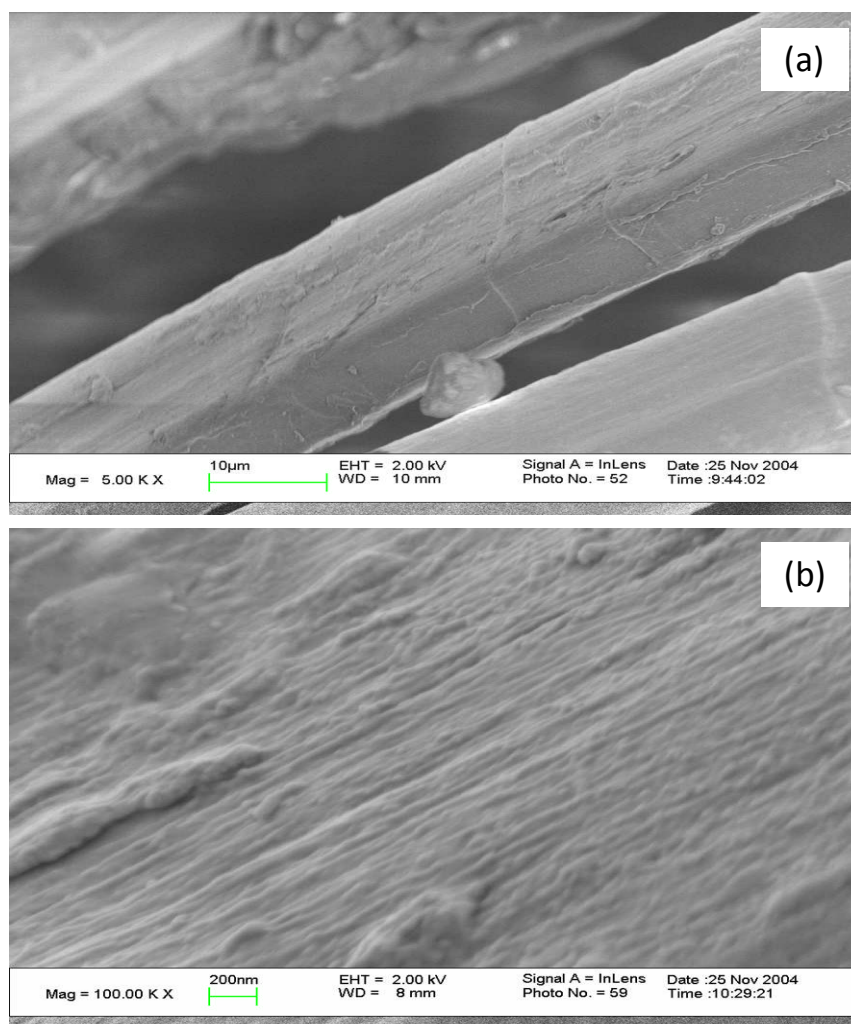


**Figure 4: SEM micrograph of raw flax fibre at (a) x5000 magnification and (b) x100,000 magnification.**

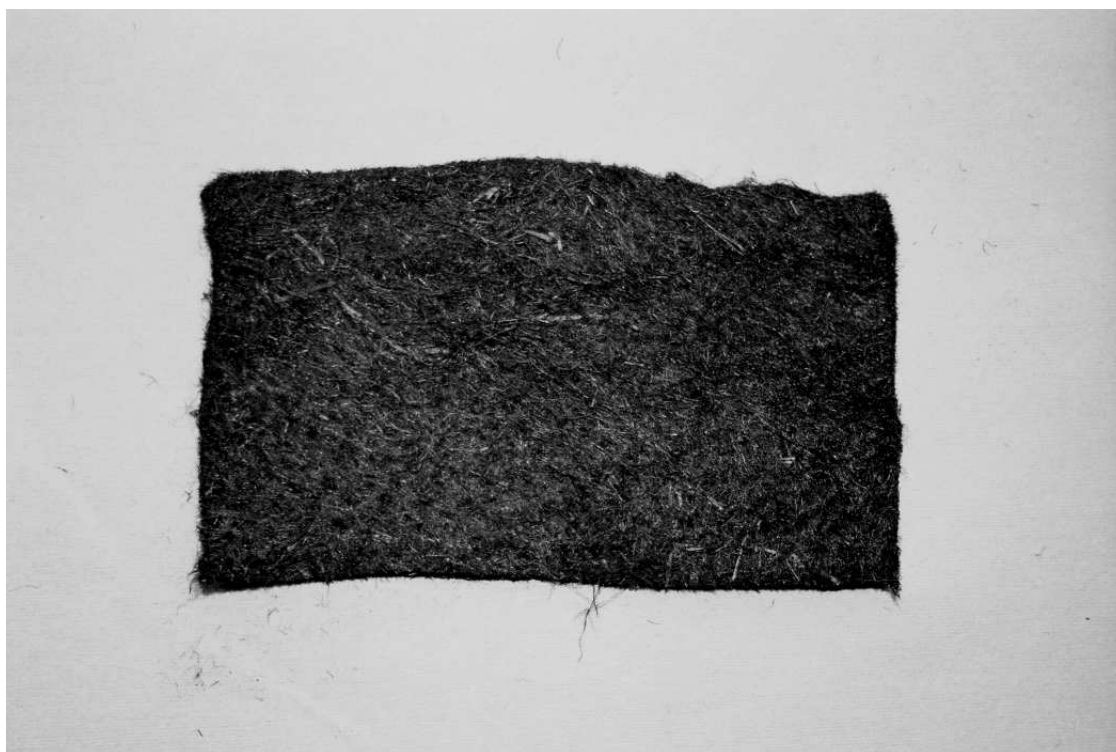


**Figure 5: Flax non-woven fabric biochar produced at a pyrolysis temperature of 800°C**

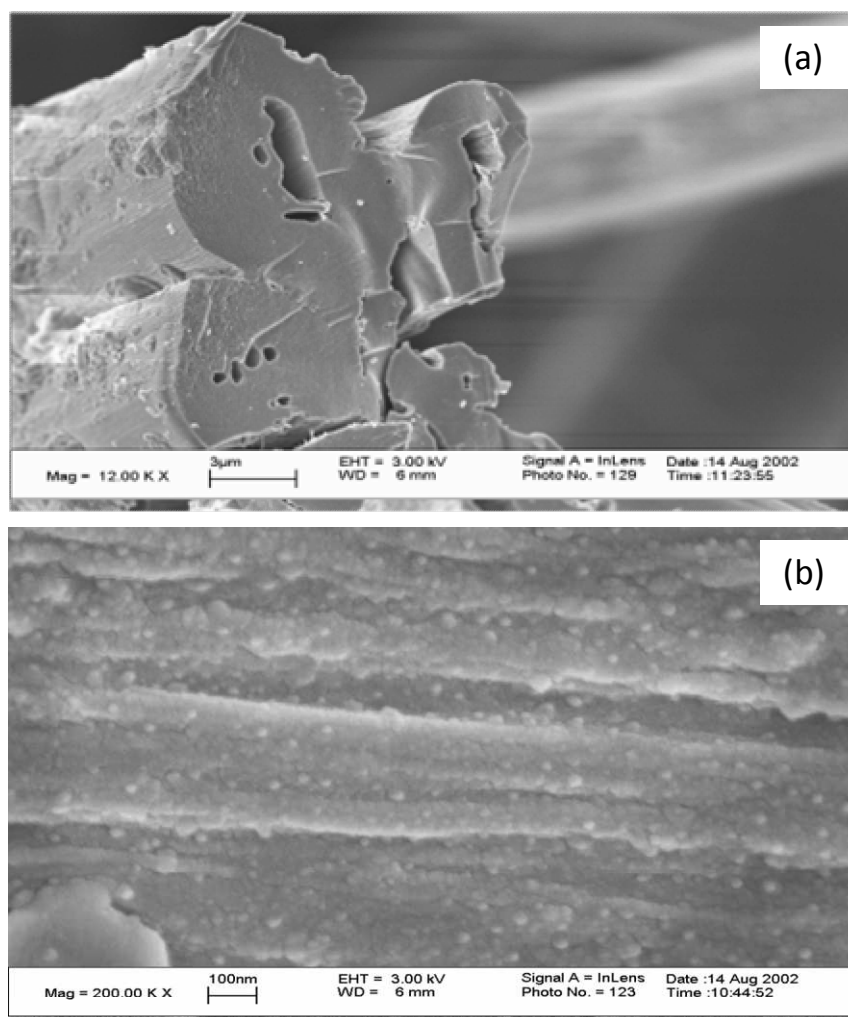


**Figure 6: SEM micrograph of flax biochar fibre surface (a) x 12000 magnification and (b) x200,000 magnification**

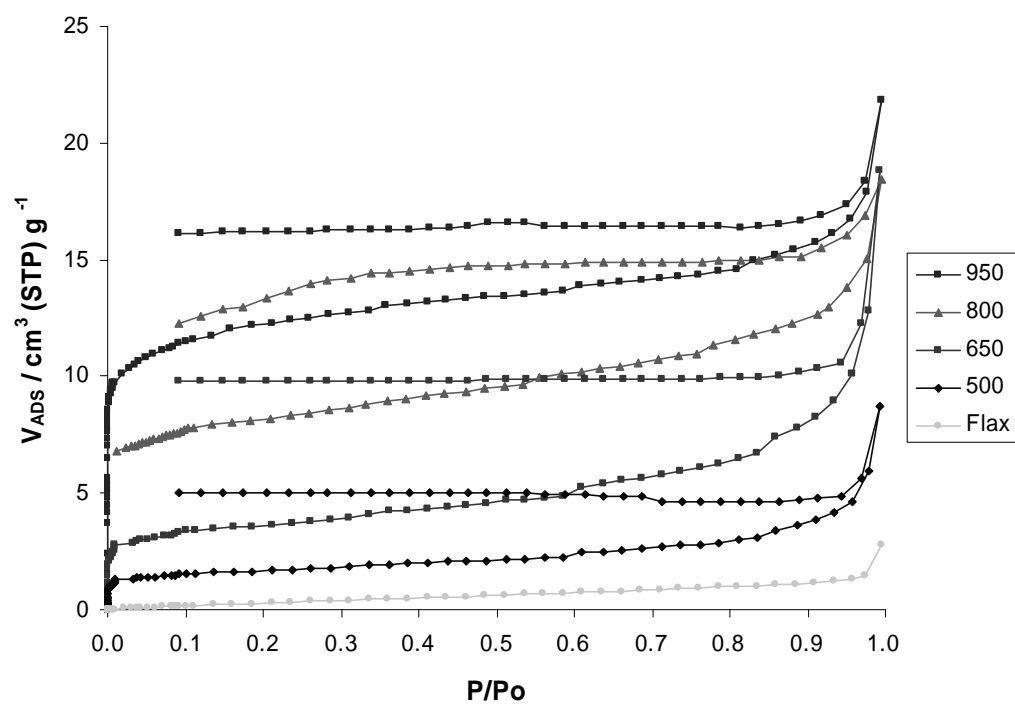


Figure 7:  $\text{N}_2$  adsorption isotherms at 77K for raw flax and biochars

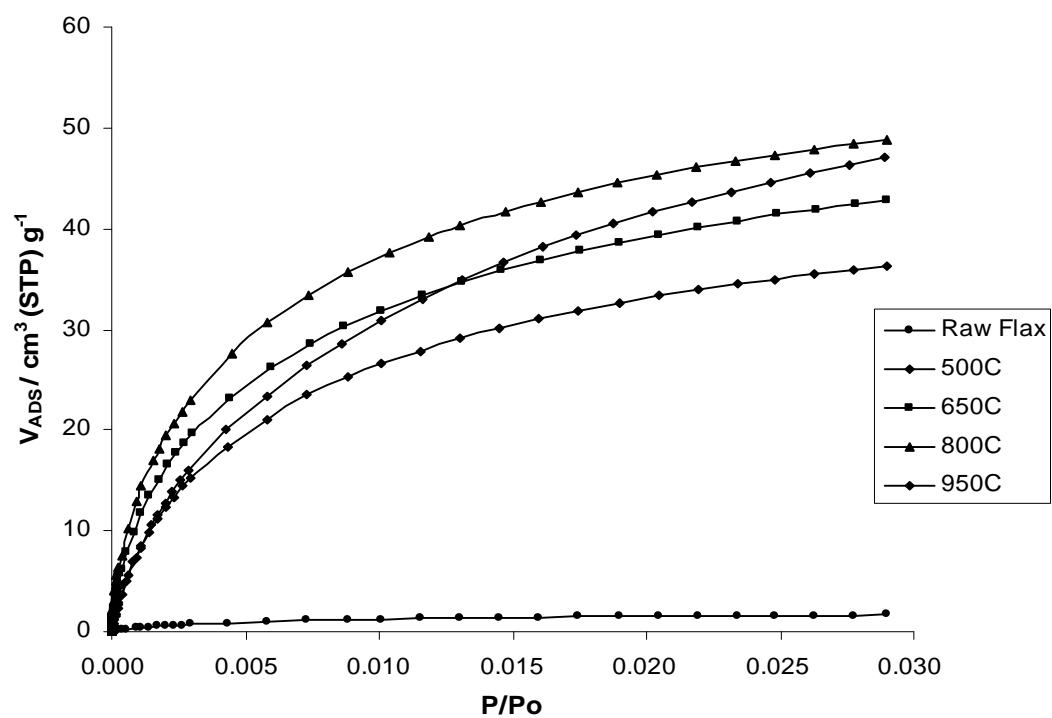


Figure 8: CO<sub>2</sub> adsorption isotherms at 273K for raw flax and biochars

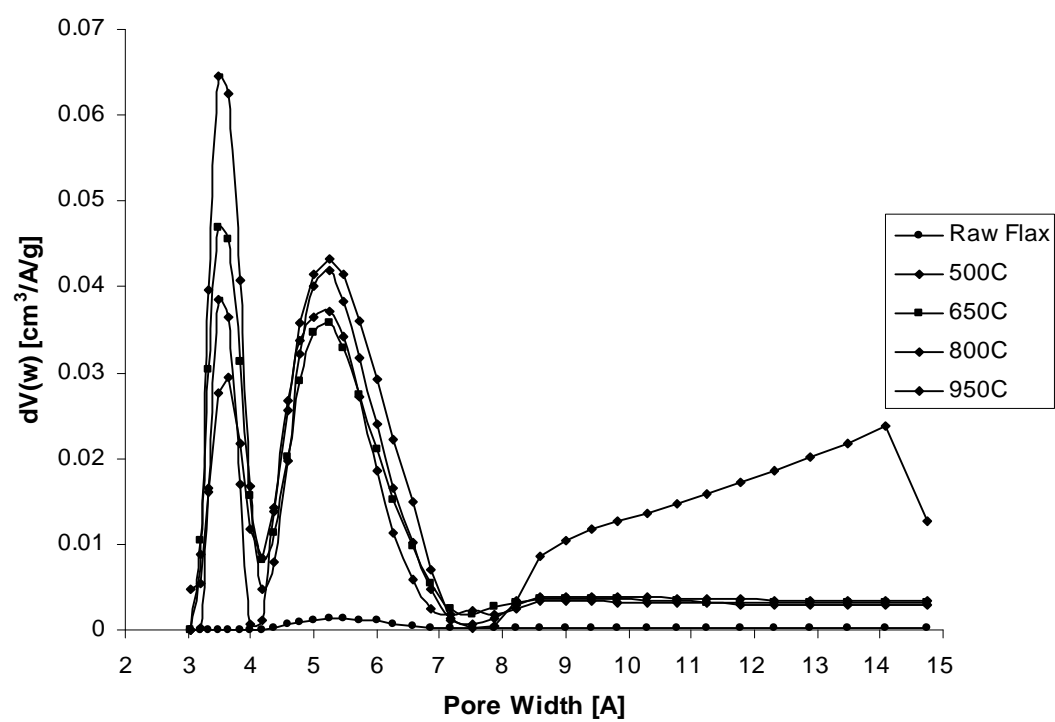
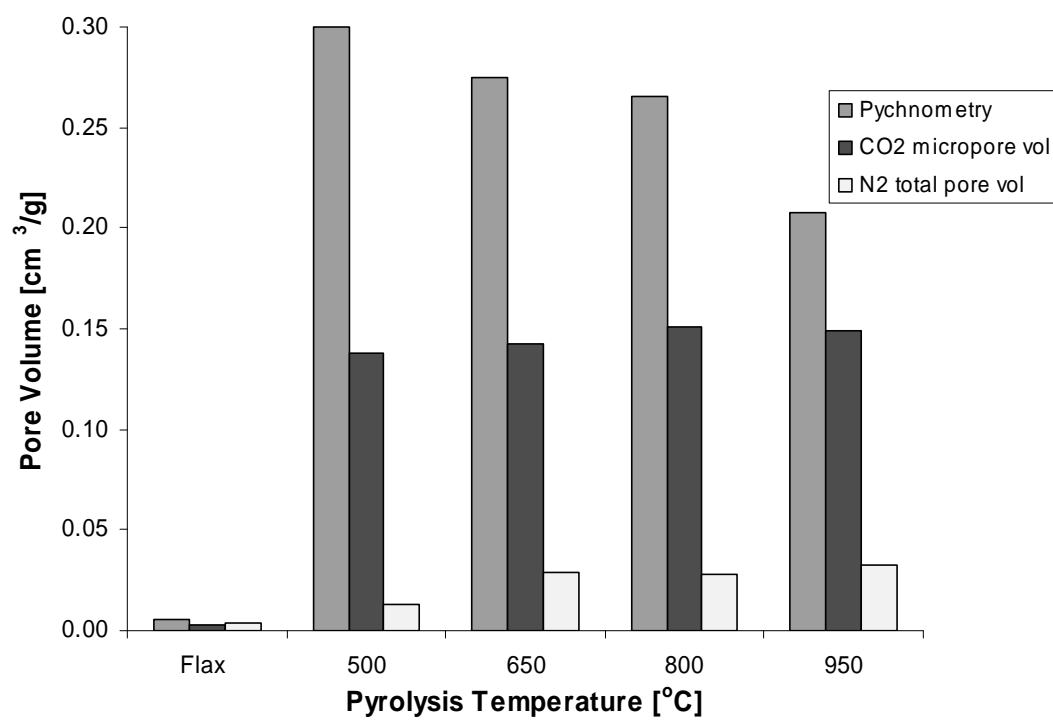


Figure 9: CO<sub>2</sub> DFT micropore size distributions for raw flax and biochars



**Figure 10: Comparison of pore volumes. Pycnometry vs gas adsorption**